Role of a Ubiquitin-Like Modification in Polarized Morphogenesis

Gunnar A. G. Dittmar,[1] Caroline R. M. Wilkinson,[1] Paul T. Jedrzejewski,[2]* Daniel Finley[1]†

Type I ubiquitin-like proteins constitute a family of protein modifiers. Here we report the identification of a posttranslational protein modifier from *Saccharomyces cerevisiae*, Hub1. Overexpression of Hub1 resulted in enhanced conjugate formation when its carboxyl-terminal residue was deleted, suggesting that mature Hub1 may be produced by proteolytic processing. In vivo targets of Hub1 conjugation included cell polarity factors Sph1 and Hbt1. In the *hub1*Δ mutant, the subcellular localization of both Hbt1 and Sph1 was disrupted, and cell polarization during the formation of mating projections was defective. Consistent with these polarization defects, the *hub1*Δ mutant was deficient in mating.

Each type I ubiquitin-like protein is, like ubiquitin, thought to be conjugated enzymatically via an isopeptide bond between its COOH-terminal carboxylate group and a lysine residue of the target protein (*1*). A distinct enzymatic system exists for each ubiquitin-like protein modifier. The functional consequences of protein modification by ubiquitin-like proteins appear to be distinct from that of ubiquitination, in that ubiquitin-like modifiers do not typically signal the degradation of their protein targets. Ubiquitin-like modifiers may serve instead as reversible modulators of protein function. For example, conjugation of the Rub1/Nedd-8 protein to the (Skp1/cullin-1/F-box protein) ubiquitin-ligase complex promotes its activity (*2–5*). Other ubiquitin-like proteins have been implicated in autophagy and nuclear transport (*6–12*).

Although functionally diverse, ubiquitin-like protein modifiers have a universal sequence feature: a glycine residue at the COOH-terminal site of conjugate formation. The *YNR032c-a/HUB1* open reading frame (ORF) of *Saccharomyces cerevisiae* exhibits slight similarity to ubiquitin (*13*) but lacks glycines proximal to its predicted COOH-terminus (Fig. 1A). Hub1 was found to be extremely well conserved in evolution (Fig. 1A), more so than any other ubiquitin-like protein (*13*, *14*). However, no specific segment of Hub1 was significantly related to ubiquitin or to any ubiquitin-like protein, and the overall identity to ubiquitin, 22%, is close to the limit of statistical significance (*15*). Hub1 may be the most divergent of ubiquitin-like modifiers, or alternatively its similarity to ubiquitin may simply reflect a shared folding topology.

To search for possible Hub1-protein conjugates, Hub1 was NH_2-terminally tagged with six histidines and an epitope (HA) from influenza hemagglutinin, then overexpressed in a *hub1*Δ deletion mutant (*13*). Little or no conjugate formation was observed. If Hub1 functions as a ubiquitin-like modifier, the amino acid at the COOH-terminal site of conjugation would presumably be evolutionarily conserved. Thus we deleted the noncon-

[1]Department of Cell Biology, Harvard Medical School, 240 Longwood Avenue, Boston, MA 02115, USA. [2]Barnett Institute, Northeastern University, Boston, MA 02115, USA.

*Present address: Genencor International, 925 Page Mill Road, Palo Alto, CA 94304, USA.
†To whom correspondence should be addressed. E-mail: daniel_finley@hms.harvard.edu

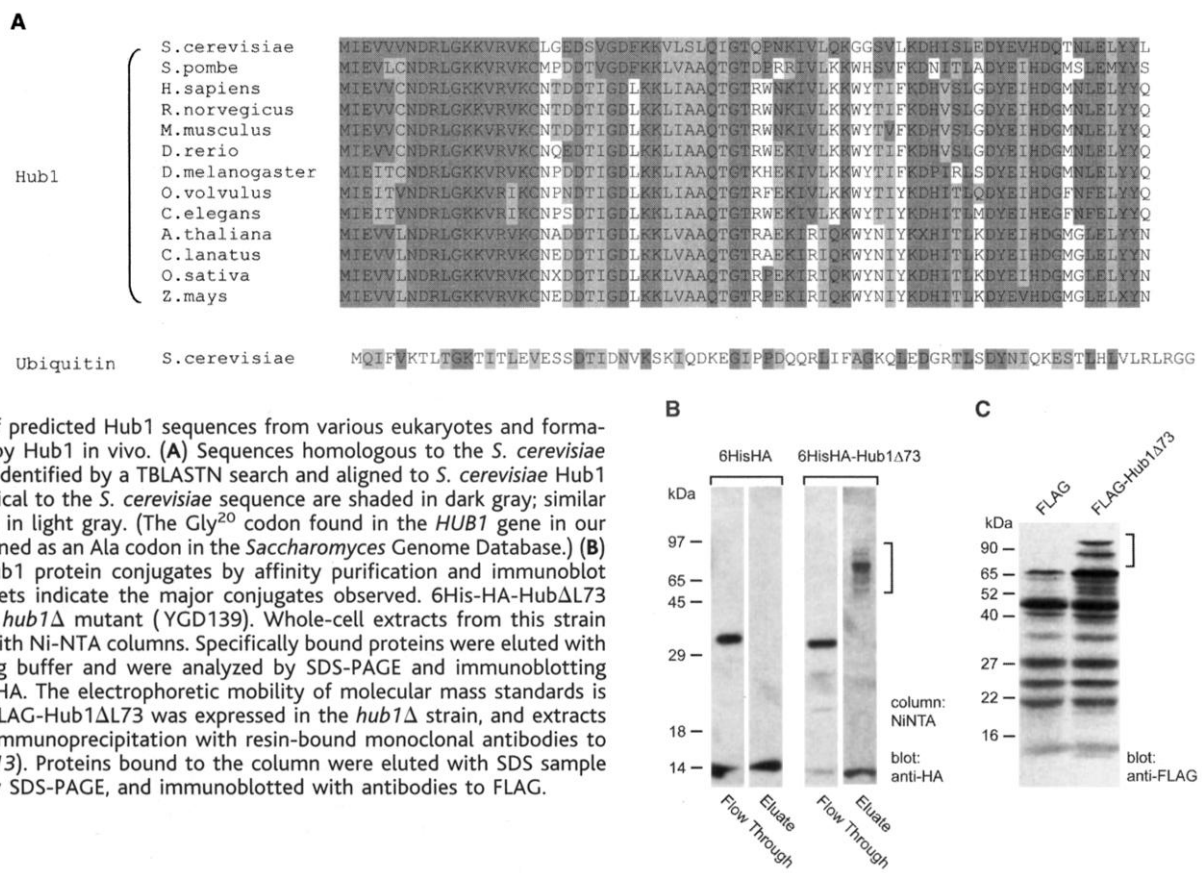

Fig. 1. Alignment of predicted Hub1 sequences from various eukaryotes and formation of conjugates by Hub1 in vivo. (**A**) Sequences homologous to the *S. cerevisiae* Hub1 protein were identified by a TBLASTN search and aligned to *S. cerevisiae* Hub1 (*14*). Residues identical to the *S. cerevisiae* sequence are shaded in dark gray; similar residues are shaded in light gray. (The Gly^{20} codon found in the *HUB1* gene in our yeast strains is assigned as an Ala codon in the *Saccharomyces* Genome Database.) (**B**) Identification of Hub1 protein conjugates by affinity purification and immunoblot analysis (*13*). Brackets indicate the major conjugates observed. 6His-HA-HubΔL73 was expressed in a *hub1*Δ mutant (YGD139). Whole-cell extracts from this strain were fractionated with Ni-NTA columns. Specifically bound proteins were eluted with imidazole-containing buffer and were analyzed by SDS-PAGE and immunoblotting with antibodies to HA. The electrophoretic mobility of molecular mass standards is shown at left. (**C**) FLAG-Hub1ΔL73 was expressed in the *hub1*Δ strain, and extracts were subjected to immunoprecipitation with resin-bound monoclonal antibodies to the FLAG epitope (*13*). Proteins bound to the column were eluted with SDS sample buffer, separated by SDS-PAGE, and immunoblotted with antibodies to FLAG.

served Leu[73] codon from the *HUB1* gene and tested for conjugate formation by the putative mature form of the protein. In contrast to the wild-type protein, Hub1ΔL73 formed multiple high-molecular-mass species (Fig. 1, B and C). Depending on experimental conditions, a number of conjugates could be observed, with molecular masses ranging from approximately 50 to 200 kD (Figs. 1 and 2).

To identify specific Hub1-protein conjugates, affinity-purified conjugate samples were analyzed by two-dimensional gel electrophoresis [isoelectric focusing followed by SDS–polyacrylamide gel electrophoresis (SDS-PAGE)] (Fig. 2A). Protein spots detectable by immunoblotting were excised from the gel and digested with trypsin. Subsequent capillary liquid chromatography electrospray mass spectrometry (cLC-ESI-MS) analysis resulted in a chromatogram from which tryptic peptides could be identified (Fig. 2B). Tandem mass spectrometric

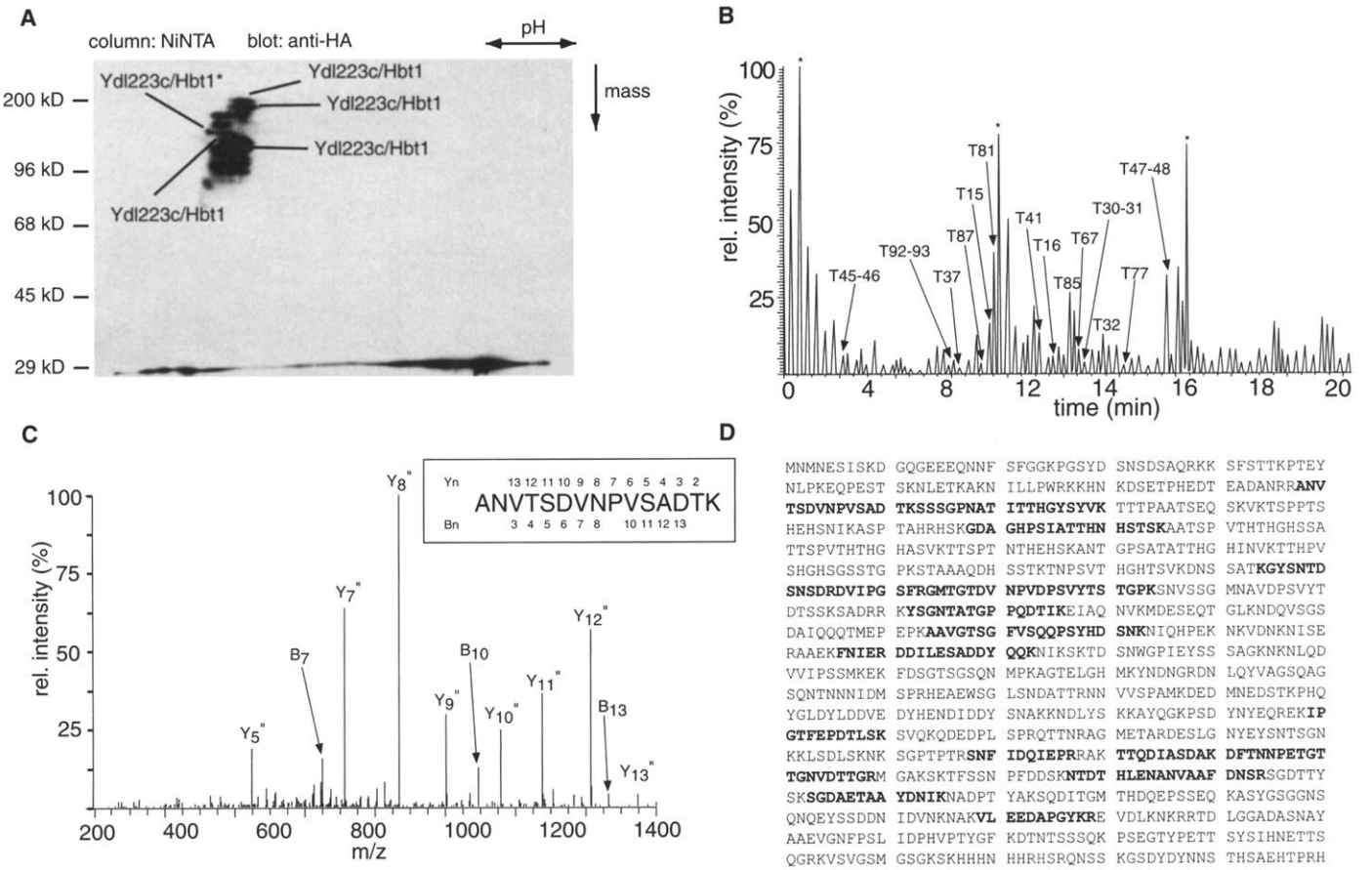

Fig. 2. Identification of Ydl223c and Sph1 as targets of Hub1 modification. (**A**) Proteins were isolated essentially as in Fig. 1B, except that isoelectric focusing (with a gradient from pH 5 to 7) was performed before SDS-PAGE (*13*). Protein were then immunoblotted and visualized with antibodies to the HA epitope. Sph1 conjugates are not seen in this approach because of the high isoelectric point predicted of Sph1 (pH 9.2). The protein spots indicated were excised from a parallel gel and analyzed by mass spectrometry. The identities of labeled spots are based on cLC-ESI-MS data as exemplified by Fig. 2, B and C. The asterisk indicates the protein spot from which the data in (B) and (C) were derived. (**B**) Chromatogram from an online capillary liquid chromatography mass spectrometric analysis of an in situ tryptic digest of the Hub1 conjugate indicated by an asterisk in (A) (*16*). Peaks are labeled with the tryptic (T) peptide number starting from the NH_2-terminus of Hbt1. Trypsin autolysis peptides are indicated with an asterisk. (**C**) Tandem MS spectrum for Ydl223c/Hbt1 peptide T15 [indicated in (B)] obtained from cLC-ESI-MS analysis. The sequence of this peptide was verified by the presence of complementary B ions (NH_2-terminus–derived fragment ions) and Y ions (COOH-terminus–derived fragment ions). (**D**) Predicted sequence of Ydl223c/Hbt1, with peptides positively identified by tandem MS shown in bold. The sequence data were used to search a yeast protein database. For the 15 peptides identified, the Sequest program (*13*) returned highly significant values (for example, Xcorr values ranging from 1.9 to 3.9 and deltaCN values ranging from 0.13 to 0.45). (**E** and **F**) Immunoblot-immunoprecipitation analyses of protein modification by Hub1 (*13*). (E) Confirmation of Hub1 modification of Ydl223c/Hbt1. (F) Hub1ΔL73, tagged with the AU1 epitope, modifies Sph1. [Both Sph1 and Ydl223c/Hbt1 were COOH-terminally tagged with 3-myc and expressed from their natural chromosomal loci (*24*) in the *hub1Δ* mutant.] The retarded mobility of Sph1 in lane 4 reflects conjugation to Hub1. (**G**) Sph1 modification by the product of the wild-type *HUB1* gene (*17*).

data were acquired, which contained sequence information for each peptide (Fig. 2C) (*16*). The 15 peptides identified allowed for unequivocal identification of the high-molecular-mass conjugate as the product of *YDL223c*, an uncharacterized ORF (Fig. 2D). Hub1 conjugation to Ydl223c in vivo was confirmed by epitope tagging (Fig. 2E), and *YDL223c* was thus renamed *HBT1* (for Hub1 target). Similar experiments identified Sph1 as a substrate (Fig. 2F) (*13*). The formation of Hub1-Sph1 conjugates does not require overexpression of these proteins nor deletion of the terminal amino acid of Hub1 (Fig. 2G) (*17*). Hbt1 and Sph1 levels were not affected in the *hub1*Δ mutant, indicating that Hub1 is unlikely to function by targeting these proteins for degradation. This conclusion was further supported by pulse-chase analysis of Sph1 turnover. The electrophoretic profile of Sph1 conjugates was consistent with modification by a single Hub1 polypeptide (Fig. 2F). The multiplicity of modified forms of Hbt1 most likely reflects in vitro instability of this protein, even in the continuous presence of 8 M urea (Fig. 2A).

Although the function of *HBT1* has not been reported, *sph1*Δ mutants exhibit defects in the formation of mating projections ("shmooing"), a process of polarized cell morphogenesis (*18*–*20*). In addition, the Sph1 protein is localized to sites of polarized growth, such as mating projections. Given the known role of Sph1 in cell polarization, the *hbt1*Δ mutant was treated with mating pheromone and examined microscopically (*21*). The mutant exhibited defects in shmoo morphology comparable in nature and in strength to those of *sph1*Δ mutants (Fig. 3A). We thus tested for a possible role of Hub1 in shmoo formation. Mating projections formed by the *hub1*Δ mutant (*21*) were indeed similar to those of *sph1*Δ and *hbt1*Δ mutants (Fig. 3A). Aberrant *hub1*Δ shmoos assumed the rounded or "peanut" morphology previously described for *sph1*Δ mutants (Fig. 3B) (*18*, *19*). The observation that the *hub1*Δ phenotype is

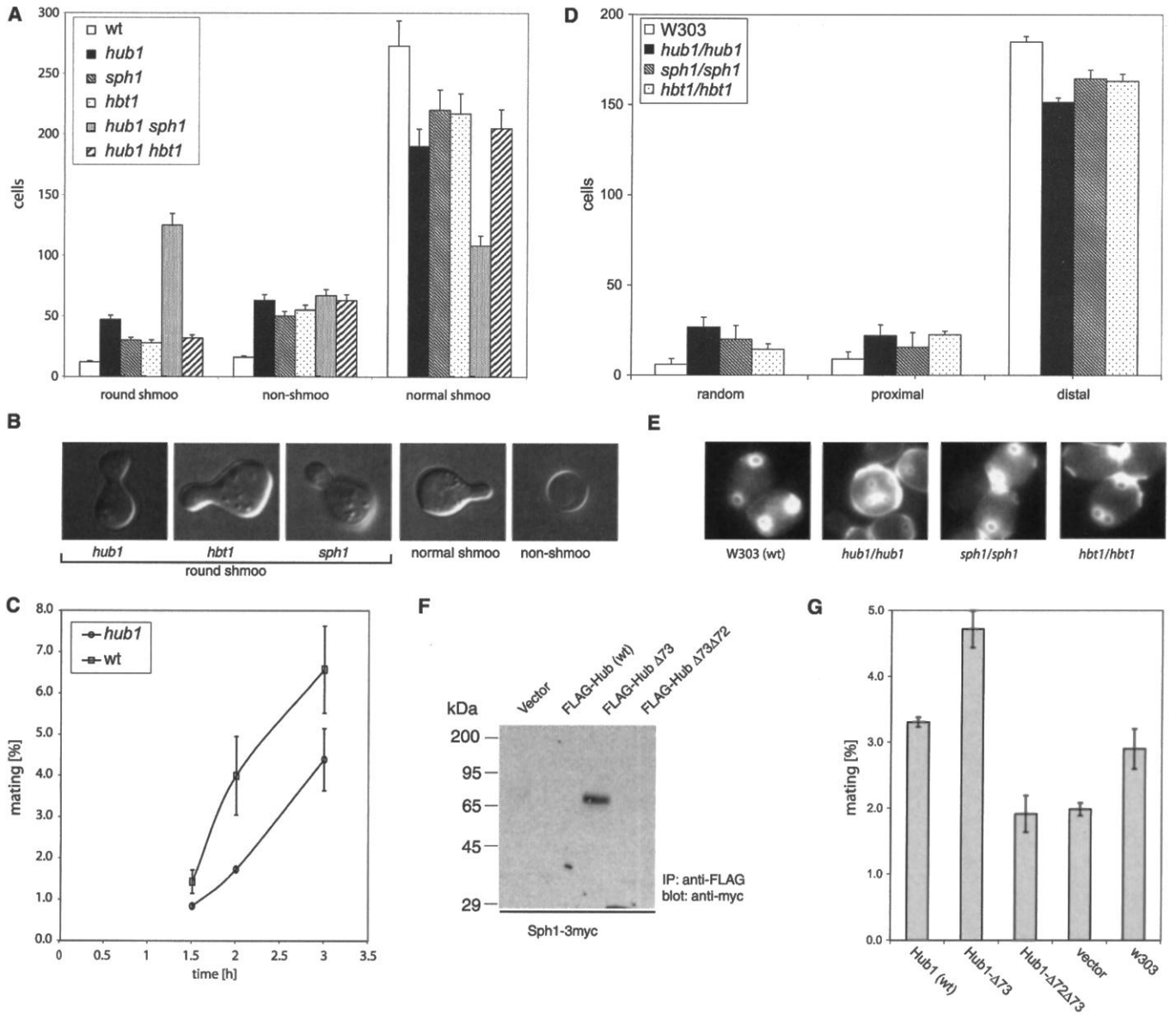

Fig. 3. *Hub1*Δ mutant cells treated with α factor show defects in morphology, mating, and bud site selection (*21*). (**A**) Cells were treated with 5 μM α factor for 3.5 hours, and their morphology was examined microscopically. Three hundred cells were scored for each strain. (**B**) Examples of the major morphological classes observed. The normal shmoo and non-shmoo shown are wild-type. (**C**) Time course of mating between two wild-type (wt) cells (W303 *MAT***a** and W303 *MAT*α) or two *hub1*Δ mutants (W303 *hub1::HIS3 MAT***a** and W303 *hub1::HIS3 MAT*α). (**D**) Budding patterns of *hub1*Δ/*hub1*Δ, *hbt1*Δ/*hbt1*Δ, and *sph1*Δ/*sph1*Δ mutants. (**E**) Examples of mutants with defective budding patterns. (**F**) Dependence of Sph1 modification on the COOH-terminus of Hub1. (**G**) *HUB1*Δ*L73* complements the mating defect of the *hub1*Δ mutant.

as strong as that of its conjugative targets raises the possibility that Hub1 might be required for the function of one or more of these proteins in cell polarization.

The *hub1*Δ mutant also exhibited reduced mating efficiency, which is probably related to its morphological defect in mating projections (Fig. 3C) (*22*). The mating defect does not reflect an inability to respond to α factor, because the characteristic G_1 cell cycle arrest induced by α factor in wild-type cells was also seen in *hub1*Δ cells.

If the function of Hub1 in the formation of mating projections involves principally covalent modification of Sph1 and Hbt1, then deletion of the *HUB1* gene should not confer an additional defect in mating projections once the *SPH1* and *HBT1* genes have been deleted. Consistent with this possibility, failure to form shmoos was no more frequent among *hub1*Δ*sph1*Δ and *hub1*Δ*hbt1*Δ double mutants than in the corresponding single mutants (Fig. 3A). The frequency of rounded shmoos was not enhanced in the *hub1*Δ*hbt1*Δ double mutant; however, an increase in rounded shmoos was observed in the *hub1*Δ*sph1*Δ double mutant. Thus, Hub1 appears to function in the formation of mating projections through the modification of its identified target proteins, and Hbt1 may be the more critical target for this phenotype.

Although the wild-type *HUB1* gene can support Hub1-Sph1 conjugate formation (Fig. 2G), an enhancement of conjugate formation results from deleting the COOH-terminal residue of Hub1 (Fig. 3F). These results suggested that Hub1 is posttranslationally processed by the removal of Leu^{73} and that processing might become rate limiting for conjugation when Hub1 is overexpressed. If the COOH-terminal processing model is correct, then deletion of one additional residue would be expected to prevent or strongly reduce conjugation. Consistent with conjugate formation through the invariant (Fig. 1A) Tyr^{72} residue, modified forms of Sph1 were eliminated or reduced in abundance when the Hub1ΔY72ΔL73 construct was tested (Fig. 3F). Comparable results were obtained with total Hub1 conjugates. Despite the different levels of conjugates formed with Hub1, Hub1ΔL73, and Hub1ΔY72ΔL73, these proteins were expressed at comparable levels. According to the mating assay, the Hub1ΔL73 protein used for conjugate identification is not functionally impaired, whereas the Hub1ΔL73ΔY72 protein shows little or no activity (Fig. 3G). These results are consistent with the model that Hub1 is conjugated to proteins through its COOH-terminus, and that the mature COOH-terminus is formed by proteolytic processing.

During G_1 phase, in vegetatively growing cells, Sph1 concentrates at the presumptive bud site (*19*). Diploid yeast exhibit a bipolar budding pattern, which is defective in *sph1*Δ/*sph1*Δ mutants (*18*, *19*). To further test for phenotypic parallels between *sph1*, *hub1*, and *hbt1* mutants, we examined their budding patterns. Both *hub1*Δ and *hbt1*Δ mutants exhibited defective bud site selection, with the severity of the defect again reflecting that of *sph1*Δ mutants (Fig. 3, D and E).

The subcellular localization of Sph1 is thought to be critical for its function (*18*, *19*). The *sph1*-like phenotype of *hub1*Δ mutants could thus reflect a role for Hub1 conjugation in Sph1 localization. To test this possibility, Sph1 was expressed as a green fluorescent protein (GFP) fusion (*23*), using its own promoter to ensure physiological expression levels. In α factor–treated cells that had elaborated a mating projection, Sph1-GFP fluorescence was found within or proximal to the mating projection (Fig. 4A). In *hub1*Δ mutants however, Sph1 was delocalized. Hbt1-GFP exhibited a localization similar to that of Sph1 and was also mislocalized in *hub1*Δ mutants. Thus, Hub1 was required for proper subcellular localization of its conjugative target proteins. These data may explain the phenotypic similarities between *hub1*, *sph1*, and *hbt1* mutants.

To test whether protein modification by Hub1 may be general to the eukaryotic kingdom, we expressed in *S. cerevisiae* presumptive *HUB1* orthologs derived from *Schizosaccharomyces pombe* and humans (*24*). Both *S. pombe* and human genes rescued the mating projection defect of the *hub1*Δ mutant (Fig. 4B). Thus, the Hub1 protein modification system has been functionally conserved during the evolution of eukaryotes, which is consistent with the very high level of identity between *HUB1* genes from *S. cerevisiae* and humans (*13*).

We have identified a pathway for protein modification that is general to eukaryotes and extremely conserved evolutionarily. The close resemblance between the shmooing and bud site selection defects observed in *hub1* mutants and those of mutants lacking either of its identified protein targets suggests that Hub1 affects cell polarity through a simple mechanism based on covalent modification of polarity-determining proteins. The mechanism by which Hub1 conjugation promotes the localization of its target proteins remains unknown. The most surprising sequence feature of Hub1 is its lack of a glycine residue at the COOH-terminal site of conjugation, previously the only absolutely conserved feature in the ubiquitin-like family of protein modifiers. If no specific sequence features are universal among ubiquitin-like modifiers, it is difficult to place an upper limit on the multiplicity of these regulators.

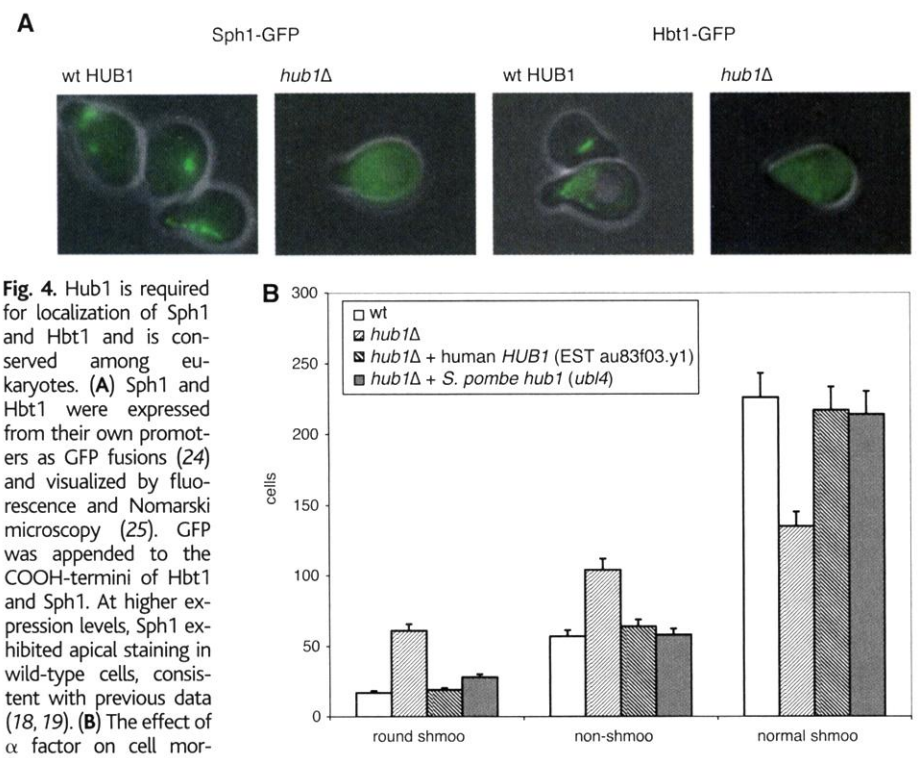

Fig. 4. Hub1 is required for localization of Sph1 and Hbt1 and is conserved among eukaryotes. (**A**) Sph1 and Hbt1 were expressed from their own promoters as GFP fusions (*24*) and visualized by fluorescence and Nomarski microscopy (*25*). GFP was appended to the COOH-termini of Hbt1 and Sph1. At higher expression levels, Sph1 exhibited apical staining in wild-type cells, consistent with previous data (*18*, *19*). (**B**) The effect of α factor on cell morphology was assayed (*21*) for wild-type cells (W303), *hub1*Δ mutants, and *hub1*Δ mutants expressing presumptive *HUB1* orthologs (Fig. 1A) from *S. pombe* and humans.

References and Notes

1. S. Jentsch, G. Pyrowolakis, *Trends Cell Biol.* **10**, 335 (2000).
2. D. Lammer *et al.*, *Genes Dev.* **12**, 914 (1998).
3. D. Liakopoulos, G. Doenges, K. Matuschewski, S. Jentsch, *EMBO J.* **17**, 2208 (1998).

4. S. Lyapina *et al.*, *Science* **292**, 1382 (2001).
5. T. Kawakami *et al.*, *EMBO J.* **20**, 4003 (2001).
7. N. Mizushima *et al.*, *Nature* **395**, 395 (1998).
8. K. Furukawa, N. Mizushima, T. Noda, Y. Ohsumi, *J. Biol. Chem.* **275**, 7462 (2000).
9. M. Hochstrasser, *Cell* **107**, 5 (2001).
10. E. S. Johnson, A. A. Gupta, *Cell* **106**, 735 (2001).
11. A. Pichler, A. Gast, J. S. Seeler, A. Dejean, F. Melchior, *Cell* **108**, 109 (2002).
12. Y. Ichimura *et al.*, *Nature* **408**, 488 (2000).
13. Supplementary Web material, including details of certain methods, is available on *Science* Online at www.sciencemag.org/cgi/content/full/295/5564/2442/DC1.
14. Sequences were identified with the TBLASTN and the FASTA tools from the GCG package. The human sequence (UBL5) is from (*25*). Expressed sequence tag (EST) sequences were translated with the translate tool (GCG). The sequence alignment was created with the CLUSTAL algorithm (*26*).
15. R. F. Doolittle, *Of URFs and ORFs: A Primer on How to Analyze Derived Amino Acid Sequences* (University Science Books, Mill Valley, CA, 1987).
16. For mass spectrometric analysis of Hub1-protein conjugates, SDS-PAGE–purified immunoprecipitates were digested in situ overnight at 37°C with modified trypsin (Promega) at an approximate ratio of 10:1 (protein:enzyme) (*27*). Digest samples were injected onto a capillary liquid chromatography–mass spectrometry system. For details, see (*13*).
17. Strain SUB62 (*28*) was modified to express a FLAG epitope at the NH_2-terminus of Hub1 and a 3myc epitope at the COOH-terminus of Sph1. Plasmid pGD132, containing FLAG-tagged *HUB1* and its flanking sequences in a YIplac211 (*29*) backbone, was constructed by PCR. This plasmid was linearized at a Bgl II site within the 3′ untranslated region of *HUB1* and chromosomally integrated, duplicating the *HUB1* gene. Strains having lost untagged *HUB1* (yGD101) were selected on 5-FOA plates and verified by sequencing. The 3myc epitope was introduced as described (*30*). Immunoprecipitations were performed as described (*13*), except that the culture volume was 1 liter and cells were harvested at an optical density at 600 nm (OD_{600}) of 4.
18. R. A. Arkowitz, N. Lowe, *J. Cell Biol.* **138**, 17 (1997).
19. T. Roemer, L. Vallier, Y.-J. Sheu, M. Snyder, *J. Cell Sci.* **111**, 479 (1998).
20. K. Madde, M. Snyder, *Annu. Rev. Microbiol.* **52**, 687 (1998).
21. For cell polarity and mating experiments, the wild-type strain was W303 [*MAT***a** (or *MAT*α) *ura3-1 leu2-3,-112 trp1-1 his3-11 ade2-1 can1-100*]. All mutant strains were congenic and carried precise deletions of the relevant coding sequence. Cell polarity was assayed with cells grown to an OD_{600} of 0.2. α factor was added to a final concentration of 5 μM, and, after a 2-hour incubation at 30°C, cells were spread onto a microscope slide and counted. For microscopy of the GFP fusion strains, cells were grown at 25°C to an OD_{600} of 0.1 to 0.2 in rich media [yeast extract, peptone, and dextrose (YPD)]. Cells were harvested by centrifugation, washed five times with sterile water, resuspended in 40% glycerol, and placed on a microscope slide. Budding patterns were assayed by Calcofluor staining of bud scars, as described (*31*). The microscope and camera assembly have been described (*32*).
22. Cells of opposite mating type were transformed with either the YCplac111 (*MAT***a**) or YCplac33 (*MAT*α) plasmids (*29*). Cells of each mating type (3×10^6) were incubated on small (Falcon 351007) YPD plates at 30°C for the time indicated. The cells were then resuspended in sterile water, and dilution series were prepared. Mating efficiency was calculated as the ratio of colonies on selective media to those on YPD.
23. Strain construction was according to (*30*). For Sph1 tagging by GFP and 3myc, the tag was added after codon Phe^{530}. Sph1 is polymorphic (*19*), and these experiments used the short form of the protein.
24. The *S. pombe HUB1*-related gene (Fig. 1A) was amplified from a cDNA library by PCR and cloned into pGD81 (*13*) under the control of the *CUP1* promoter, using restriction sites placed on the primers. The human Hub1-related gene was similarly amplified from EST au83f03.y1. The nonconserved COOH-terminal codon (Fig. 1A) was not deleted from these coding sequences.
25. J. S. Friedman, B. F. Koop, V. Raymond, M. A. Walter, *Genomics* **71**, 252 (2001).
→ J. D. Thompson *et al.*, *Nucleic Acids Res.* **22**, 4673 (1994).
→ A. Shevchenko *et al.*, *Anal. Chem.* **68**, 850 (1996).
28. D. Finley, E. Ozkaynak, A. Varshavsky, *Cell* **48**, 1035 (1987).
29. R. D. Gietz, A. Sugino, *Gene* **74**, 527 (1988).
→ M. Knop *et al.*, *Yeast* **15**, 963 (1999).
31. J. R. Pringle, *Methods Enzymol.* **194**, 732 (1991).
32. J. Lippincott, R. Li, *J. Cell Biol.* **143**, 1947 (1998).

33. We thank R. Li, C. Kaiser, and E. Elion for advice; J. Lippincott and other members of the Li lab for assistance with various experiments; and E. Elion, D. Moazed, and members of the Finley lab for critical reading of the manuscript. Supported by NIH grants GM58223 and GM62663 (to D.F.), fellowship DI724/1-1 from the Deutsche Forschungsgemeinschaft (to G.A.G.D.), a fellowship from the Medical Foundation Charles King Trust (G.A.G.D.), and an international prize traveling fellowship 058209/Z/99/Z from the Wellcome Trust (to C.R.M.W.).

18 January 2002; accepted 22 February 2002

Senescence Induced by Altered Telomere State, Not Telomere Loss

Jan Karlseder, Agata Smogorzewska, Titia de Lange*

Primary human cells in culture invariably stop dividing and enter a state of growth arrest called replicative senescence. This transition is induced by programmed telomere shortening, but the underlying mechanisms are unclear. Here, we report that overexpression of TRF2, a telomeric DNA binding protein, increased the rate of telomere shortening in primary cells without accelerating senescence. TRF2 reduced the senescence setpoint, defined as telomere length at senescence, from 7 to 4 kilobases. TRF2 protected critically short telomeres from fusion and repressed chromosome-end fusions in presenescent cultures, which explains the ability of TRF2 to delay senescence. Thus, replicative senescence is induced by a change in the protected status of shortened telomeres rather than by a complete loss of telomeric DNA.

Replicative senescence of human cells occurs as a consequence of the progressive shortening of the TTAGGG repeat tracts at chromosome ends (*1*). Human telomeres are programmed to lose ~100 base pairs (bp) per population doubling (PD), resulting in senes-

Table 1. Effect of TRF2 on telomere shortening rates and senescence setpoints.

Cell line	PD at infection	Vector*	TRF2	Setpoint
	Telomere shortening†			
IMR90	20	112	165	
IMR90	30	104	170	
IMR90	35	100	181	
IMR90	40	99	170	
IMR90–p53-175H‡	25	95	152	
IMR90–SV40 large T	30	104	162	
IMR90–HPV16-E6 + -E7	25	97	150	
BJ	80	105	197	
	Senescence setpoint§			
IMR90	20	7.1	4.4	2.7
IMR90	30	6.1	4.1	2.0
IMR90	35	6.0	3.8	2.2
IMR90	40	6.2	4.2	2.0
IMR90 p53-175H	25	5.5	3.1	2.4
BJ	80	4.7	3.5	1.2
AG02496 A-T	~20	5.6	4.9	0.7
AG04405 A-T	~20	7.0	4.8	2.2
AG03058 A-T	~20	7.3	5.8	1.5
AG03057 A-T het.	~20	7.4	5.3	2.1

*pLPC. †Base pair per end per PD. ‡Mean length of telomeric restriction fragments (in kb) in senescent cell cultures determined by genomic blotting analysis of DNA harvested 10 days after culture growth arrest. §IMR90 cells were infected with p53-175H retrovirus at PD20 and superinfected with pLPC or TRF2 viruses at PD25; the same strategy was applied for SV40 large T (at PD25) + TRF2 (at PD30) and for HPV16-E6 + -E7 (at PD20) + TRF2 (at PD25).